Role of self-trapping in luminescence and *p*-type conductivity of wide-band-gap oxides

J. B. Varley,[1] A. Janotti,[2] C. Franchini,[3] and C. G. Van de Walle[2]

[1]*Department of Physics, University of California, Santa Barbara, California 93106-9530, USA*
[2]*Materials Department, University of California, Santa Barbara, California 93106-5050, USA*
[3]*Faculty of Physics, University of Vienna and Center for Computational Materials Science, A-1090 Vienna, Austria*

We investigate the behavior of holes in the valence band of a range of wide-band-gap oxides including ZnO, MgO, In_2O_3, Ga_2O_3, Al_2O_3, SnO_2, SiO_2, and TiO_2. Based on hybrid functional calculations, we find that, due to the orbital composition of the valence band, holes tend to form localized small polarons with characteristic lattice distortions, even in the absence of defects or impurities. These self-trapped holes (STHs) are energetically more favorable than delocalized, free holes in the valence band in all materials but ZnO and SiO_2. Based on calculated optical absorption and emission energies we show that STHs provide an explanation for the luminescence peaks that have been observed in many of these oxides. We demonstrate that polaron formation prohibits *p*-type conductivity in this class of materials.

The performance of wide-band-gap oxides in electronic, photonic, and photochemistry applications is intimately related to the behavior of electrons in the lowest-energy unoccupied (conduction-band) states and holes in the highest-energy occupied (valence-band) states.[1,2]

Many of these oxides (e.g., ZnO, In_2O_3, Ga_2O_3, SnO_2, and TiO_2) exhibit unintentional *n*-type conductivity, with carrier densities and mobilities comparable to those in conventional semiconductors. The conduction-band states are derived from the metal atoms, leading to electron-related properties that vary from compound to compound. The valence-band states, on the other hand, are derived mainly from the O $2p$ orbitals and are characterized by small dispersion, large effective masses, and high density of states.

These factors are conducive to the formation of small polarons, i.e., localized holes trapped by local lattice distortions[3–6] (see Fig. 1), as opposed to the highly mobile holes that are delocalized over regions encompassing many lattice constants in conventional semiconductors. The interest in the existence of self-trapped holes (STHs) in oxides goes beyond basic research, since it is likely related to the difficulties in achieving the technologically desirable *p*-type doping of these materials and to their optical properties.

Self-trapped holes were extensively characterized in the alkali halides in which they were originally discovered and are referred to as V_k centers.[7] Electron paramagnetic resonance (EPR) and photoluminescence (PL) measurements are typically used.[3,8,9] In oxides such as α-SiO_2, localized holes associated with defects and impurities have been observed,[10,11] and trapped holes associated with aperiodic local potential fluctuations in amorphous or polycrystalline materials have also been reported.[12] Characterization of STHs not associated with defects in wide-band-gap oxides has remained elusive, however. The occurrence of isolated STHs was suggested based on EPR in TiO_2[9] and PL in Ga_2O_3.[13] Optical signatures of self-trapped excitons, which involve an electron coulombically attracted to the STH, have also been reported for MgO,[14] α-Al_2O_3,[15] and SiO_2.[16]

Although wide-band-gap oxides satisfy the criteria set by phenomenological models for the existence of STHs,[4,5]

relatively few studies based on first-principles calculations have explicitly treated trapped holes or predicted localization in otherwise perfect lattices.[17–20] The most widely used computational approach, namely, density functional theory within the local density or generalized gradient approximations (DFT-LDA or -GGA) fails in predicting such charge localization, partly as a consequence of the inherent self-interaction error in these methods. Hartree-Fock calculations for clusters have predicted the formation of STHs in α-Al_2O_3;[17] however, Hartree-Fock calculations suffer from the opposite problem of DFT-LDA/GGA, since they tend to overestimate localization.[19,21]

A new class of hybrid functionals in density functional theory overcomes the problem and provides greatly improved descriptions of charge localization.[22] In the present work we use the Heyd-Scuseria-Ernzerhof (HSE)[23] hybrid functional to study the stabilization of STHs in a set of oxide materials (ZnO, In_3O_3, Ga_2O_3, Al_2O_3, TiO_2, SnO_2, MgO, and SiO_2) that cover a wide range of crystal structures, oxygen coordinations, band gaps, and dielectric constants. We study STH stabilization by calculating energy differences between self-trapped and delocalized holes, analyze the local lattice distortions, and report on the optical absorption and emission energies associated with the trapped holes to aid in experimental characterization and identify the impact of STHs on optical properties. We show that luminescence lines observed in several of the oxides can be attributed to the formation of STH, and we offer predictions for as yet unidentified lines. In addition, our calculated energies for polaron migration indicate very low hole mobilities, thus prohibiting effective *p*-type conductivity in this class of oxides.

Our calculations are based on generalized Kohn-Sham theory with the HSE functional and the projector augmented-wave method, as implemented in the VASP code.[24,25] The parameter α that determines the amount of Hartree-Fock exchange is chosen so as to provide accurate values for band gaps, which are listed in Table I; this choice also leads to lattice constants that are within 1% of the experimental values, as summarized in the Supplemental Material[26] (see also Refs. 27–41 therein). Tests using the commonly used $\alpha = 0.25$ value show that
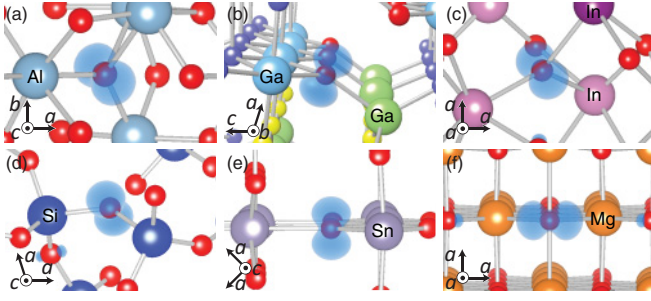
FIG. 1. (Color online) The relaxed configuration of the STH in (a) α-Al$_2$O$_3$, (b) β-Ga$_2$O$_3$, (c) bcc-In$_2$O$_3$, (d) α-SiO$_2$, (e) rutile SnO$_2$, and (f) MgO. The differently colored cations in (b) and (c) represent the inequivalent Ga and O sites in β-Ga$_2$O$_3$ and In sites in bcc-In$_2$O$_3$. The charge density isosurfaces illustrating the polaron wave function are shown at 10% of their maximum value.

our qualitative conclusions about STH stabilization are not sensitive to the choice of α, but the optimized α values are chosen for all reported stabilization energies based on their improved description of the bulk properties.

We investigate the formation of STHs by removing an electron from the valence-band maximum in a supercell and allow for low-symmetry lattice relaxations by including small random displacements of atoms around a given lattice site in the initial configuration. We use supercells consisting of 120 atoms for α-Al$_2$O$_3$ and β-Ga$_2$O$_3$, 96 atoms for ZnO, 80 atoms for bixbyite In$_2$O$_3$, 216 atoms for rutile TiO$_2$ and SnO$_2$, 162 atoms for α-SiO$_2$, and 216 atoms for MgO. We used a cutoff of 400 eV for the plane-wave basis set, and a $2 \times 2 \times 2$ mesh of special k points for the determination of atomic structures. For these structures, total energies were evaluated in a final cycle including only the Γ point to ensure proper occupation of the free hole state.

Atomic configurations and charge distribution of STHs in various oxides are shown in Fig. 1. The STH is localized mainly on a single O atom in the lattice, with a shape characteristic of an O $2p$ orbital. The stability of the STH in a given material is determined by the difference in the total energies of the localized hole η^+ (including energy cost of the local lattice distortion) and the delocalized hole h^+ in the perfect lattice, which we define as the self-trapping energy E_{ST}:

$$E_{ST} = E_{tot}[X_mO_n:h^+] - E_{tot}[X_mO_n:\eta^+] - \Delta\bar{V},$$

where $E_{tot}[X_mO_n:h^+]$ is the total energy of a supercell of the perfect crystal containing a hole in the valence-band maximum, and $E_{tot}[X_mO_n:\eta^+]$ is the total energy of the supercell containing the STH. E_{ST} contains a term $\Delta\bar{V}$ that accounts for the alignment of the average electrostatic potential between a perfect-crystal-like region in the supercell containing the STH and $\bar{V}$ in the perfect supercell. A positive E_{ST} indicates a preference for self-trapping.

The calculated E_{ST} for the various oxides is listed in Table I. Self-trapped holes are stable (i.e., lower in energy than free holes) in all of the oxides investigated here, with the exception of ZnO and α-SiO$_2$. In ZnO we find that the STH cannot be stabilized, as the atoms always relax to the ideal positions in the perfect lattice. In α-SiO$_2$ we find the STH to be metastable;
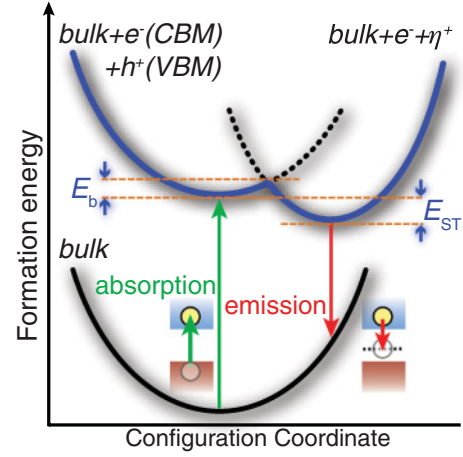

FIG. 2. (Color online) Schematic configuration coordinate diagrams showing energy as a function of the lattice distortion in the formation of a self-trapped hole (STH). The top curve illustrates the barrier E_b between a free hole (h^+) and the STH (η^+), the latter assumed to be lower in energy here by E_{ST}. The optical absorption process creates a free hole at the valence-band maximum (VBM) and an electron at the conduction-band minimum (CBM); emission results when the electron recombines with the hole, which has become localized due to self-trapping.

i.e., the STH is higher in energy than the delocalized hole, forming a local minimum configuration.

We also evaluated the energy barrier between the delocalized hole and the STH configuration by calculating total energies (based on full electronic relaxation) for a series of intermediate structures, constructed by interpolating the atomic positions between the polaronic (distorted) and the ideal (undistorted) lattice configurations,[18,21] as schematically illustrated in Fig. 2. Values are included in Table I. A finite barrier is always present to convert the delocalized hole into a STH, but the values indicate that the conversion process is probably rapid.

Ga$_2$O$_3$ displays an interesting combination of highest E_{ST} and lowest E_b among the materials studied, consistent with experimental observations of holes that are immediately self-trapped.[13] We also expect a strong tendency for STH formation in In$_2$O$_3$; no reports of self-trapped holes in In$_2$O$_3$ have appeared in the literature, to our knowledge, and we suggest this would be a fruitful area for experimental investigations given the important applications of this material as a transparent conducting oxide. STHs have also been identified in rutile TiO$_2$ at 10 K by EPR measurements under band-gap light excitation.[9]

The analysis of the optical transitions associated with STHs is based on the calculation of configuration coordinate diagrams, an example of which is shown in Fig. 2. Excitation with above-band-gap light results in electron-hole pairs; if the holes become self-trapped, emission lines with energies below the band gap can result from recombination of a conduction-band electron with a STH. Self-trapped excitons (STEs) can also form if an electron is coulombically attracted to the STH; in that case the emission energy would be further reduced by an amount equal to the exciton binding energy (not calculated here). Our calculated emission energies

TABLE I. Crystal structure, calculated and experimental band gap,[26] and calculated values for hole self-trapping energy (E_{ST}), energy barrier to self-trapping (E_b), and optical emission energy resulting from recombination of free electrons with STHs.

Oxide	Crystal structure	Band gap (eV)		Self-trapping energy E_{ST} (eV)	Barrier to trapping E_b (eV)	Emission (eV)
		Calc.	Exp.			
TiO_2	Rutile	3.13	3.03	0.11	0.11	2.04
SnO_2	Rutile	3.50	3.6	0.07	0.22	2.27
α-Al_2O_3	Corundum	8.82	8.8	0.13	0.19	7.25
β-Ga_2O_3	Monoclinic	4.83	4.9	0.53	0.10	3.10
In_2O_3	Bixbyite	3.04	2.9	0.25	0.14	1.51
ZnO	Wurtzite	3.34	3.4	–	–	–
MgO	Rocksalt	7.95	7.9	0.01	0.20	6.80
α-SiO_2	α-quartz	8.73	8.9	−0.05	0.21	7.70

are included in Table I. Due to the large lattice distortions associated with the STH, the emission lines are predicted to be much broader than photoluminescence lines arising from band-edge transitions; i.e., recombination involving STHs is characterized by broad bands, large Stokes shifts, and a strong temperature dependence, all indicative of large electron-phonon coupling.

Our calculated STH emission energy of 6.8 eV in MgO is in very good agreement with the 6.9 eV luminescence peak attributed to self-trapped excitonic recombination in MgO.[14] Similarly for Al$_2$O$_3$, our calculated emission energy of 7.25 eV is close to the observed luminescence peak at 7.5 eV assigned to STE recombination.[15] The agreement found for these well-established cases gives us confidence that our calculated emission energies can be used to identify the source of luminescence lines in other materials, where attributions have been lacking.

For instance, it has been widely reported that Ga$_2$O$_3$ exhibits a broad UV luminescence (UVL) centered around 3.1 eV.[42,43] This has typically been attributed to bound excitons, but with a band gap of 4.83 eV, it seems highly unlikely that this luminescence originates from band-edge recombination. Based on the excellent agreement between our calculated emission line at 3.10 and the 3.12 eV value experimentally observed in undoped single-crystal Ga$_2$O$_3$,[43] we conclude that the UVL is due to STHs, supporting previous suggestions.[42,43]

For SnO$_2$, our calculated STH emission of 2.27 eV likely explains the broad green luminescence observed in highly resistive single crystals under UV illumination, peaked at 2.38 eV at low temperature.[44] Interestingly, we find that the STH in In$_2$O$_3$ would result in infrared emission centered at 1.51 eV, a wavelength range that, to our knowledge, has not been probed in optical studies of this material.

The formation of STHs has profound consequences for p-type conductivity in oxide semiconductors. Even if shallow acceptors can be identified and incorporated (which has

proven very challenging), the resulting holes would become self-trapped and exhibit very poor mobilities. An estimate for the barrier for STH migration can be obtained by taking the sum of E_{ST} and E_b. Using Ga$_2$O$_3$ as a representative case, we have investigated the migration of STHs in more detail by calculating the energy along a linearly interpolated path between initial and final polaron configurations along the crystallographic b axis, resulting in a barrier of 0.40 eV. Assuming an activated process we can estimate a polaron mobility based on the Einstein relation,[45] obtaining $\mu \simeq 10^{-6}$ cm^2/V s at room temperature.[26,46] Such a low value indicates that, even if holes could be introduced in these wide-band-gap oxides (i.e., the Fermi level shifted to the vicinity of the VBM), no significant p-type conductivity can be achieved.

In summary, we have presented hybrid functional calculations for self-trapped holes in a variety of technologically relevant wide-band-gap oxides. STHs are stable in nearly all of the studied oxides, except for ZnO. We note that STHs can be further stabilized by the presence of impurities or native defects; this could also provide a stabilization mechanism in case STHs are higher in energy than free holes in the perfect crystal. We have also reported luminescence energies associated with the STH, finding good agreement with experiment in some well-established cases and allowing us to propose attributions for as yet unidentified PL peaks in others. We conclude that STH formation is a fundamental property of many oxide systems, which profoundly affects their electrical and optical performance and poses an insurmountable obstacle to the achievement of p-type conductivity.

[1] M. Grundmann, H. Frenzel, A. Lajn, M. Lorenz, F. Schein, and H. von Wenckstern, Phys. Status Solidi A **207**, 1437 (2010).

[2] E. Fortunato, D. Ginley, H. Hosono, and D. C. Paine, MRS Bull. **32**, 242 (2007).

[3] N. Itoh and A. M. Stoneham, *Materials Modification by Electronic Excitation* (Cambridge University Press, Cambridge, UK, 2001).

[4] A. M. Stoneham, J. Gavartin, A. L. Shluger, A. V. Kimmel, D. Muñoz Ramo, H. M. Rønnow, G. Aeppli, and C. Renner, J. Phys. Condens. Matter **19**, 255208 (2007).

[5] A. L. Shluger, K. P. McKenna, P. V. Sushko, D. Muñoz Ramo, and A. V. Kimmel, Modell. Simul. Mater. Sci. Eng. **17**, 084004 (2009).

[6] C. Franchini, G. Kresse, and R. Podloucky, Phys. Rev. Lett. **102**, 256402 (2009).

[7] T. G. Castner and W. Könzig, J. Phys. Chem. Solids **3**, 178 (1957).

[8] D. Schoemaker, Phys. Rev. B **7**, 786 (1973).

[9] S. Yang, A. T. Brant, and L. E. Halliburton, Phys. Rev. B **82**, 035209 (2010).

[10] O. F. Schirmer, Solid State Commun. **18**, 1349 (1976).

[11] T. J. L. Jenkin, J. Koppitz, O. F. Schirmer, and W. Hayes, J. Phys. C **20**, L367 (1987).

[12] D. L. Griscom, J. Non-Cryst. Solids **352**, 2601 (2006).

[13] T. Harwig and F. Kellendonk, J. Solid State Chem. **24**, 255 (1978).

[14] Z. A. Rachko and J. A. Valbis, Phys. Status Solidi B **93**, 161 (1979).

[15] B. Namozov, M. Fominich, R. Zakharchenya, and V. Myurk, Phys. Solid State **40**, 837 (1998).

[16] C. Itoh, K. Tanimura, N. Itoh, and M. Itoh, Phys. Rev. B **39**, 11183 (1989).

[17] P. W. M. Jacobs and E. A. Kotomin, Phys. Rev. Lett. **69**, 1411 (1992).

[18] P. Zawadzki, K. W. Jacobsen, and J. Rossmeisl, Chem. Phys. Lett. **506**, 42 (2011).

[19] S. Sicolo, G. Palma, C. Di Valentin, and G. Pacchioni, Phys. Rev. B **76**, 075121 (2007).

[20] D. Muñoz Ramo, A. L. Shluger, J. L. Gavartin, and G. Bersuker, Phys. Rev. Lett. **99**, 155504 (2007).

[21] S. Lany, Phys. Status Solidi B **248**, 1052 (2011).

[22] B. G. Janesko, T. M. Henderson, and G. E. Scuseria, Phys. Chem. Chem. Phys. **11**, 443 (2009).

[23] J. Heyd, G. E. Scuseria, and M. Ernzerhof, J. Chem. Phys. **118**, 8207 (2003); **124**, 219906 (2006).

[24] G. Kresse and J. Furthmüller, Phys. Rev. B **54**, 11169 (1996). M. Marsman, J. Paier, A. Stroppa, and G. Kresse, J. Phys. Condens. Matter **20**, 064201 (2008).

[25] P. E. Blöchl, Phys. Rev. B **50**, 17953 (1994); G. Kresse and D. Joubert, *ibid*. **59**, 1758 (1999).

[26] See Supplemental Material at http://link.aps.org/supplemental/10.1103/PhysRevB.85.081109 for values of α, lattice constants, band gaps, and formation enthalpies.

[27] D. T. Cromer and K. Herrington, J. Am. Chem. Soc. **77**, 4708 (1955).

[28] W. H. Strehlow and E. L. Cook, J. Phys. Chem. Ref. Data **2**, 163 (1973).

[29] J. Pascual, J. Camassel, and H. Mathieu, Phys. Rev. Lett. **39**, 1490 (1977).

[30] *CRC Handbook of Chemistry and Physics* edited by D. R. Lide, (CRC Press, Boca Raton, FL, 2005), pp. 850–856.

[31] A. A. Bolzan, C. Fong, B. J. Kennedy, and C. J. Howard, Acta Crystallogr. Sect. B **53**, 373 (1997).

[32] M. Nagasawa and S. Shionoya, Phys. Lett. **22**, 409 (1966).

[33] R. E. Newnham and Y. M. D. Haan, Z. Kristallogr. **117** (1962).

[34] R. H. French, J. Am. Ceram. Soc. **73**, 477 (1990).

[35] S. Geller, J. Chem. Phys. **33**, 676 (1960).

[36] M. Mohamed, I. Unger, C. Janowitz, R. Manzke, Z. Galazka, R. Uecker, and R. Fornari, J. Phys. Conf. Ser. **286**, 012027 (2011).

[37] M. Marezio, Acta Crystallogr. **20**, 723 (1966).

[38] P. D. C. King, T. D. Veal, F. Fuchs, C. Y. Wang, D. J. Payne, A. Bourlange, H. Zhang, G. R. Bell, V. Cimalla, O. Ambacher, R. G. Egdell, F. Bechstedt, and C. F. McConville, Phys. Rev. B **79**, 205211 (2009).

[39] O. Madelung, *Semiconductors: Data Handbook*, 3rd ed. (Springer-Verlag, New York, 2004).

[40] G. A. Lager, J. D. Jorgensen, and F. J. Rotella, J. Appl. Phys. **53**, 6751 (1982).

[41] G. L. Tan, M. F. Lemon, D. J. Jones, and R. H. French, Phys. Rev. B **72**, 205117 (2005).

[42] T. Harwig, F. Kellendonk, and S. Slappendel, J. Phys. Chem. Solids **39**, 675 (1978).

[43] K. Shimamura, E. G. Víllora, T. Ujiie, and K. Aoki, Appl. Phys. Lett. **92**, 201914 (2008).

[44] J. P. Fillard and M. de Murcia, Phys. Status Solidi A **30**, 279 (1975).

[45] N. A. Deskins and M. Dupuis, Phys. Rev. B **75**, 195212 (2007).

[46] B. Liu, M. Gu, and X. Liu, Appl. Phys. Lett. **91**, 172102 (2007).